Available online at www.CivileJournal.org

Civil Engineering Journal

Vol. 5, No. 3, March, 2019

The Responses of an End-Bearing Pile to Adjacent Multipropped Excavation: 3D Numerical Modelling

Dildar Ali Mangenjo [a*], Naeem Mangi [b], Hemu [a]

[a] *Department of Civil Engineering, Mehran University of Engineering and Technology, Shaheed Zulfiqar Ali Bhutto Campus, Khairpur Mir's, Sindh, Pakistan.*

[b] *Department of Civil Engineering, Quaid-e-Awam University of Engineering, Science and Technology, Nawabshah, Sindh, Pakistan.*

Received 28 December 2018; Accepted 05 March 2019

Abstract

It is well recognised that superstructure load is transferred to surrounding soil through piled foundation. Consequently, the high stress regime (stress bulb) is generated surrounding of the pile. On the other hand, the excavation in the ground inevitably results in the ground movement due to induced-stress release. These excavations are sometimes inevitable to be constructed adjacent to existing piled foundations. This condition leads to a big challenge for engineers to assess and protect the integrity of piled foundation. This research presents three-dimensional coupled consolidation analyses (using clay hypoplastic constitutive model which takes account of small-strain stiffness) to investigate the responses of an end-bearing pile due to adjacent excavation at different depths in soft clay. The effects of excavation depths (i.e., formation level) relative to pile were investigated by simulating the excavation near the pile shaft (i.e., case S) and next to (case T). It was revealed that the maximum induced bending moment in the pile after completion of excavation in all the cases is much less than the pile bending moment capacity (i.e. 800 kNm). Comparing the induced deflection of the end-bearing pile in the case T, the pile deflection in case S is higher. Moreover the piles in cases of S and T were subjected to significant dragload due to negative skin friction.

Keywords: Excavation; End-Bearing Pile; 3D Coupled Consolidation; Soft Clay.

1. Introduction

It is well recognised that a pile foundation transfers the load of superstructure to surrounding soil which is adjacent to pile shaft as well as underneath the piled foundation. Consequently, the high stress regime (stress bulb) is generated surrounding of the pile [1]. On the other hand, the excavation in the ground inevitably results in the ground movement due to induced-stress release [2]. To cope with transportation problems in congested cities in the world like Hong Kong, Shanghai, London etc, underground transportation systems (involving tunnels for metros, excavations of metro stations and basement to facilitate inhabitants in the buildings for parking) have been developed. These excavations are sometimes inevitable to be constructed adjacent to existing piled foundations. This condition leads to a big challenge for a geotechnical engineer to assess and protect the integrity of piled foundation.

Finno et al. [1] and Goh et al. [2] reported case studies in granular soil and Alluvium residual soil respectively. They demonstrated that lateral soil movements due to excavation can be detrimental to adjacent piles. In both the reported case studies, piles toe level was much deeper than the excavation level and they reported only the lateral behaviour of piles. Apart from field monitoring, a number of centrifuge tests were also conducted to investigate the response of single

* Corresponding author: dildarali72@gmail.com

http://dx.doi.org/10.28991/cej-2019-03091267

pile (Ong et al. [23]) and pile group in soft Kaolin clay (Ong et al. [24]). They concluded that the induced bending moment and lateral deflection of piles were highly influenced by distance from wall and pile head condition. In studies, lateral response of end bearing piles without initial applied load was reported. In reality, piled foundation in soft clay behave as floating pile group and subjected to initial applied load from superstructure. In the presence of initial applied load, soil surrounding the pile foundation experience higher stress level before the commencement of adjacent excavation. Leung et al. [10-12] conducted centrifuge tests to investigate the effects of an un-propped excavation on the behaviours of nearby single piles and pile groups in dry dense Toyoura sand. It was found that the distance from the pile to the retaining wall and pile head conditions had a large influence on the induced pile bending moment and lateral deflection. Ng et al. [21] reported the results of three centrifuge tests which were carried out to study the effects of a multi-propped deep excavation in-flight on the behaviour of single piles in dry Toyoura sand. Piles were laterally restrained in terms of rotation and deflection right at or above ground surface in the three different tests. It was concluded that lateral restraints imposed on the pile head have a significant influence on induced pile bending moment. Induced bending moment due to excavation can exceed the pile bending capacity. Poulos and Chen [25] developed design charts to compute the lateral behaviour of a single pile adjacent to deep excavation in soft ground. They performed two staged analysis considering plane strain conditions and linear elastic soil model. Similar work was conducted by Liyanapathirana and Nishanthan [14] using finite element method. In both these studies lateral response of single pile was investigated.

The settlement behaviour of pile and development of excess pore water pressure and consolidation settlement were not investigated. Korff et al [8] proposed an analytical method to investigate reduction of capacity and increase in settlement of a nearby pile during excavation. It was reported that pile settlement due to excavation depends on the percentages of end bearing and shaft friction of the pile, the soil movement pattern, and the distribution of the maximum shaft friction with depth. However, shaft resistance in these methods is calculated on the assumption that horizontal stress acting on the piles does not change during excavation. This assumption may not be valid and the pile settlement may be underestimated using the preceding methods, leading to a non-conservative prediction. Shakeel and Ng [28] carried out three-dimensional coupled consolidation analysis is conducted to gain insight into the response of a (2×2) floating pile group adjacent to deep excavation in soft clay. By using a validated finite element model, the influence of the excavation depth, pile length, pile group location from excavation, the supporting system stiffness, soil state and permeability, and working load are systematically studied. The analysis revealed that the maximum settlement occurs when the pile group is founded at the excavation level and at a distance of 0.75 times the excavation depth, although the induced bending moment is insignificant. In contrast to pile group settlement, tilting is significant when it gets closer to the wall and minimum at a distance of 0.75 times the excavation depth. Zhang et al. [27] carried out the finite element analyses considering soil of the hardening small strain (HSS) constitutive model to establish the excavation-induced pile behaviors by varying the depth of excavation, pile diameter, pile length, pile distance away from the excavation, pile-head fixity, unsupported depth of excavation and axial loadings exerted on the pile head. Soomro et al [26] conducted parametric study to investigate the responses of floating pile to adjacent excavation at different depths. They concluded that the pile responses to excavation depend upon formation level of the excavation as well as the embedded depth of the wall. With different wall depth in each case, the induced settlement, lateral displacement and bending moment in the pile at the same stage of the excavation was different in the three cases.

Most of previous studies focused on lateral response of the piled foundation to excavation. Besides this, the location of an excavation depth relative to a pile foundation has not been studied systematically. The effects of excavation on the behaviour of piles (i.e., induced settlement and axial forces along the pile length) were rarely reported.

It is well understood that the stress-strain relationship of soils is highly nonlinear even at very small strain. The stiffness of most soils decreases as strain increases and depends on the recent stress or strain history of the soil [2, 3]. Owing to non-linear soil behaviour, an excavation can cause reduction in the stiffness of the ground. To obtain a satisfactory numerical model of single pile responses to excavation-induced stress relief, the analysis needs to take account of the small strain non-linearity of soil.

This study aims at systematically investigating the effects of different excavation depths on a floating and an end-bearing pile. A three-dimensional coupled consolidation numerical parametric study was carried out to analyse the responses of the single piles to the excavations. Lateral displacement, bending moment, induced lateral forces and axial load distribution along the pile and stress changes during excavation are reported and discussed.

2. Research Methodology

Three-dimensional finite element analysis was carried out to investigate the responses of an end-bearing pile to excavation-induced stress release. Figure 1 shows the flow chart which illustrates the step by step methodology adopted in this study.

With the prime objective of investigating the effects of the different excavation depths relative to an end-bearing pile, a three-dimensional coupled consolidation numerical parametric study was carried out. Two different final excavation

depths (H_e) relative to the pile length (L_p) namely near the pile shaft (Case S), adjacent to the pile toe (Case T)) are taken in this parametric study. The final depth of the excavation (H_e) has been adopted as 12 m and 18 m in cases of S and T, respectively. The embedded length (L_p) and diameter (d_p) of the pile are 18 m and 0.8 m, respectively. The modelled pile represents a cylindrical reinforced concrete (grade 40, reinforcement ratio = 1) with a bending moment capacity of 800 kNm.

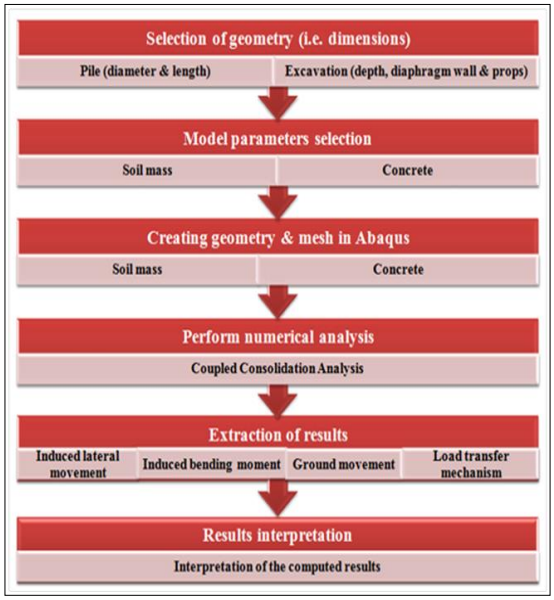

Figure 1. Configuration of a typical numerical run representing case of S; (a) elevation view (b) plan view

Figure 2(a) shows the elevation view of the configuration of numerical simulation in case of S. The clear distance between diaphragm wall and the pile is 3.0 m. The excavation was supported by 0.6 m thick diaphragm wall.

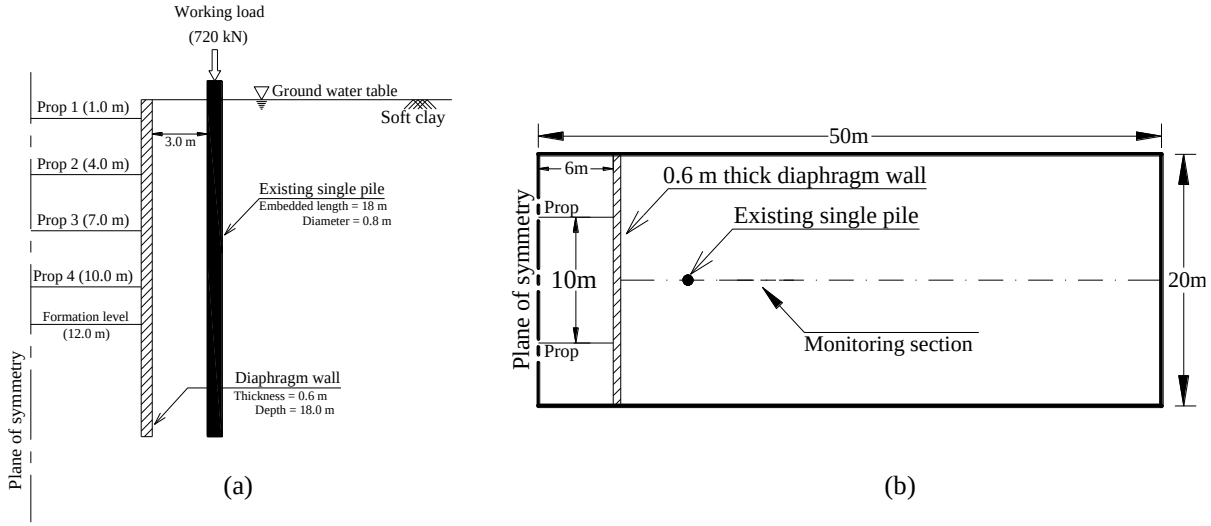

Figure 2. Configuration of a typical numerical run representing case of S; (a) elevation view (b) plan view

The ratio of wall penetration depth to excavation depth is typically 0.5-2 in engineering practice [6, 7], and thus a value of 0.5 is adopted in this study. The props are used to support the diaphragm wall with a vertical spacing of 3 m. The props are modelled as soft with axial rigidity of 81×10^3 kNm [7]. Horizontal spacing of props is 10 m.

It is worth noting that, in reality, high-rise buildings are unlikely to be built on a single pile. This hypothesised study is a more virtual case [4-6]. This simplification is made to understand the settlement and load transfer mechanism clearly. Figure. 1(b) illustrates the plan view of the configuration of the numerical simulation. The length of the excavation is 12 m. Due to symmetry, only half of the excavation was simulated. A monitoring section was selected at the transverse centreline of the excavation. Table 1 summarises numerical simulations conducted in this study.

Table 1. Summary of numerical simulations

Numerical simulation ID	Excavation depth; He (m)	Diaphragm wall depth (m)	Remarks
S	12.0	18.0	Formation level near pile shaft
T	180	24.0	Formation level next to pile toe

2.1. Finite Element Mesh And Boundary Conditions

The finite element program Abaqus will be used in this study. The size of the mesh for each numerical runs will be taken as 50× 20×40 m as shown in Figure 3. Eight-noded hexahedral brick elements are used to model the soil, the pile and the diaphragm wall, while two-noded truss elements are adopted to model the props.

Roller and pin supports are applied to the vertical sides and the base of the mesh, respectively. Therefore, movements normal to the vertical boundaries and in all directions of the base are restrained. The water table is assumed to be at ground surface. Initially, the pore water pressure distribution is assumed to be hydrostatic. Free drainage is allowed at the top boundary of the mesh.

The pile-soil and wall-soil interface is modelled as zero thickness by using duplicate nodes. The interface is modelled by the Coulomb friction law, in which the interface friction coefficient (μ) and limiting displacement (γ_{lim}) are required as input parameters. A limiting shear displacement of 5 mm is assumed to achieve full mobilization of the interface friction equal to μ×p', where p' is the normal effective stress between two contact surfaces and a typical value of μ for a bored pile of 0.35 is used in all analyses [9]. The excavation process will be simulated by deactivating soil elements inside excavation zone. In the meantime, the truss elements representing the props will be activated.

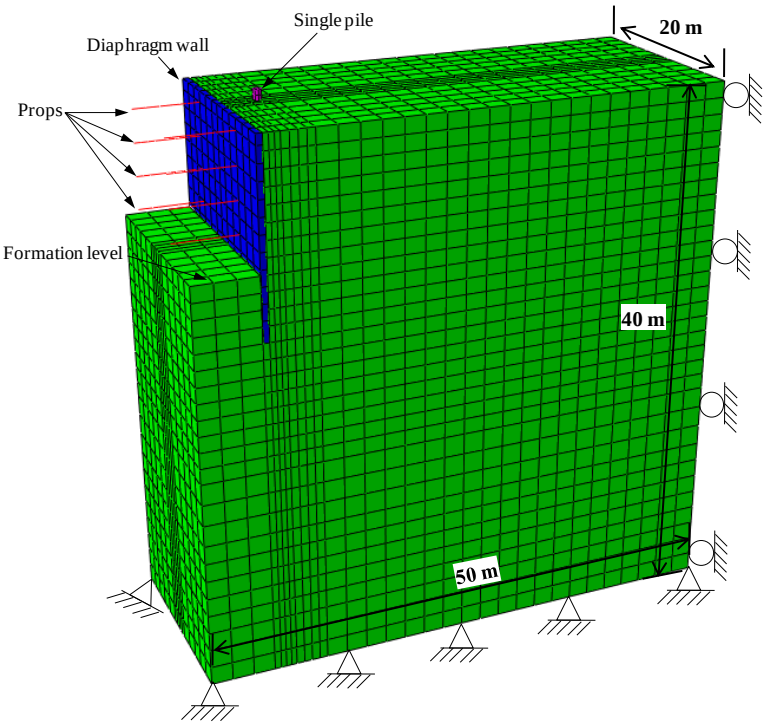

Figure 3. Finite element mesh and boundary conditions of a typical numerical analysis (i.e. S)

2.2. Constitutive Model And Model Parameters Used In Finite Element Analyze

The unique feature of basic hypoplastic model is to capture nonlinear behaviour within range of strain level of medium to large (due to monotonic loading) of granular material [15, 16]. The basic model consists of five parameters $(N, \lambda^*, \kappa^*, \varphi_c$ and $r)$. The position and the slope of normal compression line in the space of $\ln(1+e)$ versus $\ln p'$ (where e is the void ratio, and p' is the mean effective stress) is representing by the parameters N and λ^*, respectively. The parameter κ^* represents the slope of the isotropic unloading line in the same plane. φ_c is the friction angle at critical state, and the parameter r controls the large strain shear modulus. Mašín [17] further implemented the concept of intergranular strain to improve the basic hypoplastic model. To take into consideration of the strain and path dependency of soil stiffness, five additional parameters (required by intergranular strain) were included into the basic model. These five additional parameters are R, β_r, χ, m_T and m_R in which R is elastic range and β_r and χ determine the rate of stiffness degradation. The remaining parameters m_T and m_R regulate the initial shear modulus, respectively.

The hypoplastic clay model [15] with small strain stiffness has been implemented in the commercial finite element software package Abaqus through a user-defined subroutine.

The parameters (i. e. , N, λ^*, κ^* and φ_c) for kaolin clay have been widely reported in the literature. Based on these four known parameters, the parameters which are r (i.e., controlling soil stiffness at medium to large-strain levels) and at small-strain levels (i.e, R, β_r, χ, m_T and m_R) were calibrated against existing experimental data of kaolin clay. The model parameters at small- strain and large-strain ranges are calibrated against the measured stress–strain relationships and the measured stiffness degradation curves in kaolin clay, respectively.

The coefficient of lateral earth pressure at rest, K_o is estimated by Jáky [14]'s equation:

$$K_0 = (1 - sin\varphi') \quad (1)$$

All model parameters for soft clay are summarised in Table 2.

Table 2. Model parameters of kaolin clay adopted in the parametric study

Description	Parameter
Effective angle of shearing resistance at critical state: ϕ'	22º
Parameter controlling the slope of the isotropic normal compression line in the ln(1 + e) versus lnp plane, λ*	0.11
Parameter controlling the slope of the isotropic normal compression line in the ln(1 + e) versus lnp plane, κ*	0.026
Parameter controlling the position of the isotropic normal compression line in the ln(1 +e)–lnp plane, N	1.36
Parameter controlling the shear stiffness at medium- to large- strain levels, r	0.65
Parameter controlling initial shear modulus upon 180° strain path reversal, m_R	14
Parameter controlling initial shear modulus upon 90° strain path reversal, m_T	11
Size of elastic range, R	1×10^{-5}
Parameter controlling the rate of degradation of the stiffness with strain, β_r	0.1
Parameter controlling degradation rate of stiffness with strain, χ	0.7
Initial void ratio, e	1.05
Dry density (kg/m^3)	1136
Coefficient of permeability, k (m/s)	1×10^{-9}

Since end-bearing piles are resting on hard stratum (i.e. rock). The rock was modelled as an elastic material. The modulus of elasticity and Poisson's ration of rock were taken as 70 GPa and 0.3, respectively [21].

The concrete pile, the diaphragm wall and the props were assumed to be linear elastic with Young's modulus of 35 GPa and Poisson's ratio of 0.25. The unit weight of concrete was assumed to be 24 kN/m^3. The parameters for the rock and the piles and the diaphragm wall are summarised in Table 3.

Table 2. Model parameters of kaolin clay adopted in the parametric study

Mechanical properties	Rock	Concrete
Young's Modulus, E (GPa)	70	35
Poisson's ratio, ν	0.3	0.3
Density, ρ (kg/m^3)	2560	2400

2.3. Constitutive Model And Model Numerical Modelling Procedure

The numerical analysis modelling procedure for a typical case (i.e. case S) is summarized as follows:

Step 1: Set up the initial boundary and initial stress conditions (i.e., static stress conditions with varying K_0 =0.63).

Step 2: Activate the brick elements representing single pile (modeled as "wished-in-place").

Step 3: Apply the working load (determined from numerical pile load test) on the pile.

Step 4: Allow excess pore pressure, which generated in result of application of working load on the pile, to dissipate.

Step 5: Activate the brick elements representing the diaphragm wall.

3. Interpretation of Computed Results

3.1. Induced Lateral Displacement in the Pile Due to Excavation

Figure 4 shows the lateral pile displacement induced due to excavation in both case S and T. The positive values of the pile deflection indicate the lateral movement of the pile towards excavation side. It can be seen from the figure that the pile head displaced away laterally from the excavation side in each case. Because the toe of the end-bearing pile is resting on the hard stratum, negligible movement of the pile toe of the end-bearing toe was induced due to excavation. Comparing the induced deflection of the end-bearing pile in the case T, the pile displacement in case S is higher than that in case T. This result can be ascribed to soil displacement due to excavation-induced stress release. The horizontal component of soil displacement vectors towards excavation in case S is slightly higher than that of case T. The maximum deflection induced at the pile head is approximately 15 mm (2.0% d_p) in both cases. In contrast to end-bearing pile, Soomro et al [26] reported that the pile toe of the friction pile deflected towards the excavation side and the pile head displaced away from the excavation in both the cases. Furthermore the excavation-induced deflection profile reveals that the pile has rotated counter-clockwise about an axis perpendicular to the plane of the figure. The centre of rotation is approximately at Z/L_p=0.25 in both the cases. This is because of excavation-induced stress release and soil displacement (flow) towards excavation. The soil displaced towards excavation near the toe of the friction pile resulting in the movement of the toe in both cases. A similar pile deflection profile during an adjacent excavation of the friction pile was observed by Liyanapathirana and Nishanthan (2016). The maximum deflection of the pile after the completion of the excavation was computed as 40 (5.0% d_p) and 32 mm (4.0% d_p) in cases of S and T, respectively.

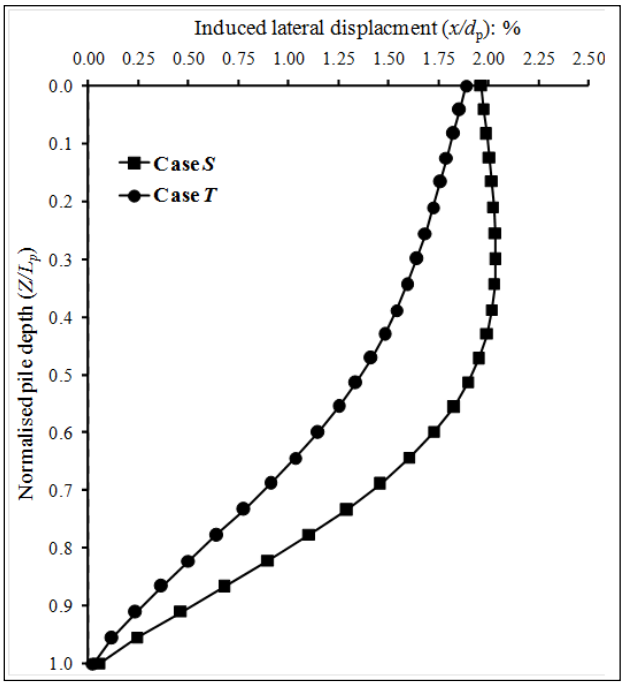

Figure 4. Induced pile lateral displacement due to excavation

3.2. Induced Bending Moment Profile along the Pile

Figure 5 illustrates bending moment profile along the pile length induced after completion of the excavation in each of case S and case T. A positive bending moment indicates that the pile side facing the excavation is subjected to compressive stresses.

It can be observed from the figure that there was no any bending moment observed at the head of the pile because of no any constraint at the pile head. However, significant bending moment could be induced at the head of the end-bearing pile if large pile head deflection induced due to excavation (discussed in previous section) is constrained. In case of S, the negative bending moment was induced along the upper portion of the pile (Z/L_p < 0.9). However, the portion of the pile near the pile toe was subjected to positive bending moment. This is because the pile was subjected to lateral force due to soil movement towards excavation and the constraint of movement of the pile toe (i.e. no any pile toe deflection as shown in Figure 3) in the hard stratum. The maximum negative and positive bending moment of 260 kNm and 350 kNm were computed at Z/L_p = 0.64 and the pile toe, respectively.

In case of T, the induced bending moment profile is similar to that in case of S. However, the maximum bending moment (of magnitude 125 kNm) induced at Z/L_p = 0.55 is smaller than that in case of T. This is because of the vertical component of displacement vector of soil due to deeper excavation in case of T is slightly higher than that in case of S.

Comparing the induced bending moments of floating reported by Soomro et al [26] and end-bearing piles in case of S, negative bending moment was induced along the entire pile length of both types of piles in case T. Moreover, the bending moment reduces as excavation became deeper in case of T (i.e. formation level H_e = 18 m). The reason for this bending profile of both the piles can be attributed to the embedded depth of the wall which makes the vertical component of the soil displacement vector higher than that of horizontal component in case of S. The maximum bending moment induced of 42 kNm at Z/L_p = 0.7 in floating pile.

It can be seen that the maximum induced bending moment of pile after completion of excavation in all the cases is much less than the pile bending moment capacity (i.e. 800 kNm). Therefore, the most critical issue to be considered in excavation-soil-pile problem is relatively large lateral displacement of the pile. This conclusion may not be applicable to scenarios in which the ground conditions or stiffness of excavation system (i.e. wall and prop stiffness) are different from those adopted in this study.

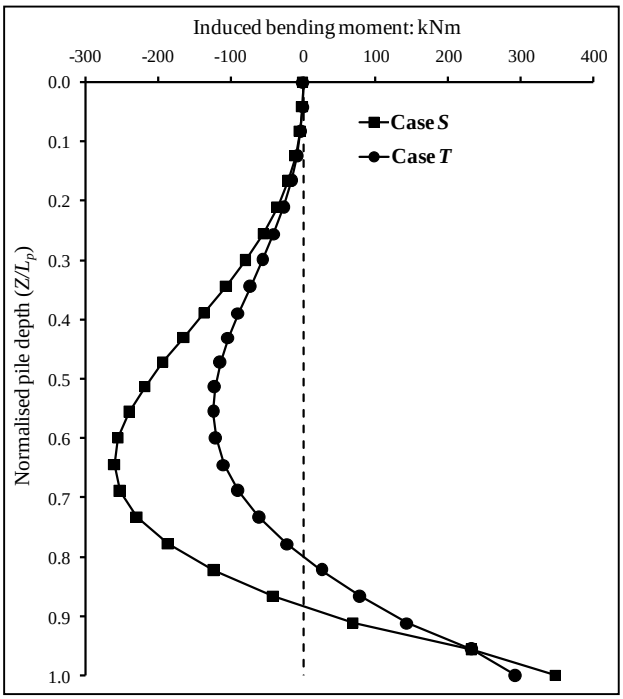

Figure 5. Induced bending moment in the pile due to excavation

3.3. Computed Ground Deformation Mechanism and Deviatoric Strain

Figure 6 (a) and (b) illustrates the excavation-induced soil displacement in the ground in cases of S and T, respectively. In addition, excavation-induced shear strain contours are also superimposed in the figure.

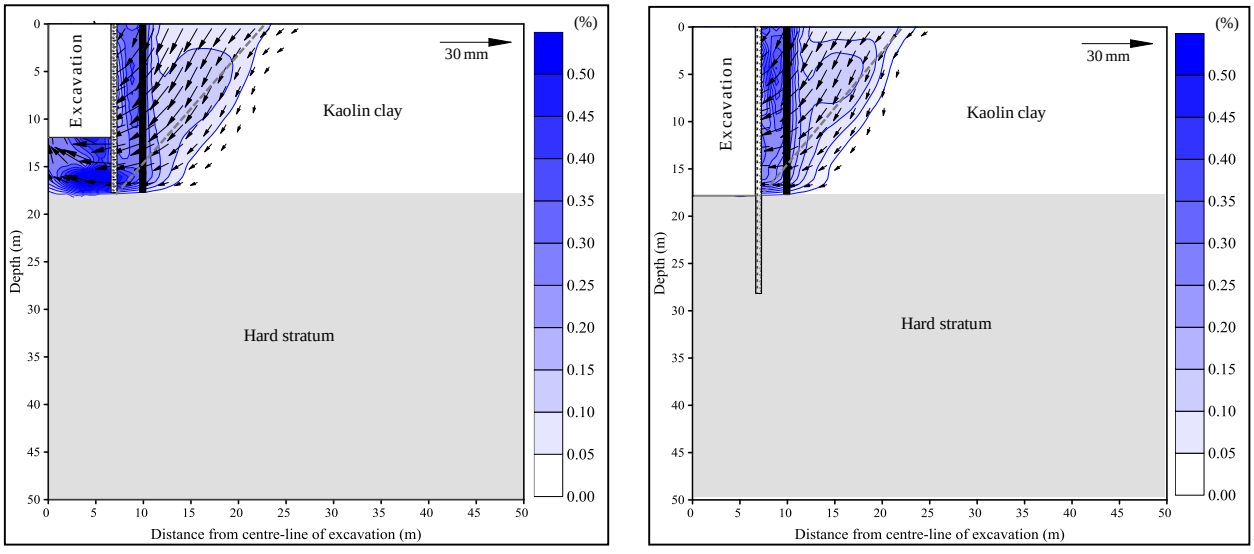

(a) (b)

Figure 6. Computed soil displacement vectors and incremental deviatoric strain contours in the pile (a) Case S; (b) Case T

It can be seen from the figure that the direction of soil displacement in retained side is towards excavation. As a result the upper part of the piles in both cases displaced towards excavation side (see Figure 3). Moreover, soil heave at excavation side in case of S. However, no heave is observed on excavation side in case of T. Consequently, the induced lateral deflection and bending moment in end-bearing pile profiles in case of T were similar to that in case of S but lesser magnitude.

3.4. Load Transfer Mechanism along the Pile Due to Excavation

To explore load transfer mechanism along the piles due to adjacent excavation, the changes in axial load distribution and mobilised shaft resistance along the pile length are discussed in this section

3.4.1. Load Transfer Mechanism Along the Pile Due to Excavation

Figure 7 shows the axial load distribution along the normalised pile length (i.e. Z/L_p) below the ground surface after excavation in case of S and T. For reference, axial load distribution after application of the working load (before excavation) is included. Because of the toe of the end-bearing pile on hard stratum, 100% of the working load transferred to the toe of end-bearing pile. This means that zero shaft resistance were mobilised along the end-pile length.

It can be seen from the figure that on the completion of the excavation, axial load distribution in the pile due to excavation altered significantly in each case. The axial load increased along the entire pile length. By inspecting the load distribution after excavation, it can be seen that negative shaft resistance along the entire pile length was mobilised in each case. This is because of the significant ground movement due to excavation (see Figure 5) and the pile toe resting on the hard stratum (due to which no any settlement induced). This suggests that the pile was subjected to "dragload" by the surrounding soil. This led to increase the end-bearing resistance increased significantly. Owing to the excavation, the en-bearing resistance increased to 42% and 57% in case of S and T, respectively. In contrast to changes in axial load distribution in floating piles due to excavation reported by Soomro et al [26], the load distribution along the end-bearing piles altered significantly in each case. The axial load increased along the entire pile length. By inspecting the load distribution after excavation, it can be seen that negative shaft resistance along the entire pile length was mobilised in each case. This is because of the significant ground movement due to excavation (see Fig. 8) and the pile toe resting on the hard stratum (due to which no any settlement induced). This suggests that the pile was subjected to "dragload" by the surrounding soil. This led to increase the end-bearing resistance increased significantly. Owing to the excavation, the en-bearing resistance increased to 42% and 57% in case of S and T, respectively.

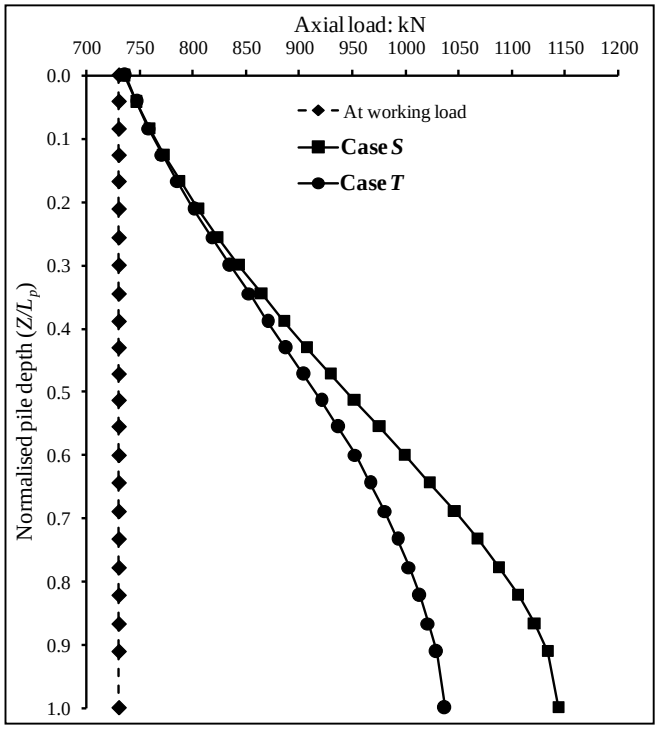

Figure 7. Axial load distribution in the pile before and after excavation

3.4.2. Load Mobilised Shaft Resistance on Completion of Excavation

To substantiate the discussion in the previous section, the mobilised shaft resistance in the end-bearing piles after the application of the working load (i.e., before excavation) and excavation in cases of S and T is shown in Figure 8. In the

figure, the depth below the ground surface (*Z*) is normalised by the pile length (L_p). The computed average mobilised unit shaft resistance *f(Z)* at various depths was calculated based on the following equation:

$$f(Z) = \frac{\Delta Q_{(Z)}}{s.\Delta Z} \quad (2)$$

Where ΔQ is the difference between the computed axial loads at two consecutive depths, ΔZ is the vertical distance between the two consecutive depths, and s is the perimeter of the pile.

It is seen that after applying a load, zero shaft resistance mobilised in the pile, as expected. Inspecting the mobilised shaft resistance changes in the due to excavation, it can be seen that the soil movement due to excavation caused negative skin friction (NSF) mobilization along the entire pile length in each of cases (i.e. S and T). This implies that the pile is 'dragged' down by the surrounding soil which settles due to excavation. This observation is because of the end-bearing pile resting on the hard stratum stopping to settle. However, the induced ground movement surrounding the pile dragged the pile down resulting NSF. This led to increase end-bearing resistance (see Figure 6) to maintain equilibrium of the pile after excavation. The maximum negative shaft resistance of 12.4 kPa was induced at the mid of the end-bearing pile (Z/Lp =0.5).

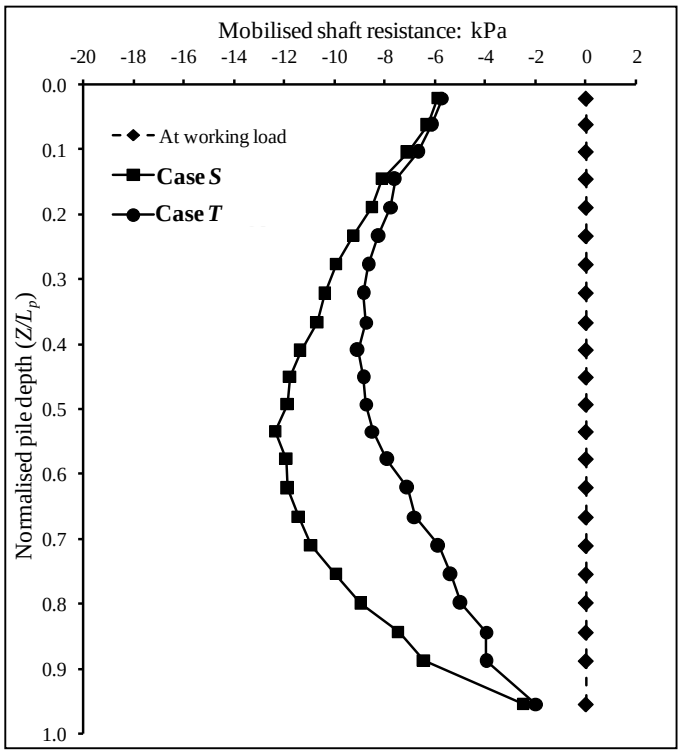

Figure 8. Mobilised shaft resistance along the pile before and after excavation

4. Conclusions

This study investigate the responses of a end-bearing pile due to different excavation depths in saturated soft Kaolin clay using 3D coupled consolidation analysis. The effects of excavation depths relative to pile were investigated by simulating the excavation near the pile shaft (i.e. case S) and next to toe (i.e. case T). Based on ground conditions, different configurations and method of excavation modelled, the following conclusions can be drawn

- Negligible movement of the pile toe of the end-bearing toe was induced due to excavation. Because the toe of the pile is resting on the hard stratum. Comparing the induced deflection of the end-bearing pile in the case T, the pile deflection in case S is higher.
- The negative bending moment was induced along the entire pile length of both types of piles in case T). The maximum induced bending moment in both types of piles after completion of excavation in all the cases is much less than the pile bending moment capacity (i.e. 800 kNm).
- On the completion of the excavation, piles were subjected to significant dragload. The downward load transfer mechanism was observed in end-bearing pile resulting in the end-bearing resistance increment of 42% and 57% in case of S and T, respectively.

6. Acknowledgement

The authors would like to thank Mehran University of Engineering & Technology and Quaid-e-Awam University of Engineering, Science & Technology for the support.

7. Conflicts of Interest

The authors declare no conflict of interest.

8. References

[1] Finno, R J, Lawrence, S A, Allawh, N F, and Harahap, I S. "Analysis of performance of pile groups adjacent to deep excavation". Journal of Geotechnical and Geoenvironmental Engineering, ASCE; 117 (June 1991): 934–955. doi:10.1061/(ASCE)0733-9410(1991)117:6(934).

[2] Goh, A T C, Wong, K S, Teh, C I, and Wen, D. "Pile response adjacent to braced excavation". Journal of Geotechnical and Geoenvironmental Engineering, ASCE; 129 (April 2003): 383–386. doi:10.1061/(asce)1090-0241(2003)129:4(383).

[3] Gudehus, Gerd, Angelo Amorosi, Antonio Gens, Ivo Herle, Dimitrios Kolymbas, David Mašín, David Muir Wood, et al. "The Soilmodels.info Project." International Journal for Numerical and Analytical Methods in Geomechanics 32, no. 12 (August 25, 2008): 1571–1572. doi:10.1002/nag.675.

[4] Hong, Y., and Charles W.W. Ng. "Base Stability of Multi-Propped Excavations in Soft Clay Subjected to Hydraulic Uplift." Canadian Geotechnical Journal 50, no. 2 (February 2013): 153–164. doi:10.1139/cgj-2012-0170.

[5] Hsieh, Pio-Go, and Chang-Yu Ou. "Shape of Ground Surface Settlement Profiles Caused by Excavation." Canadian Geotechnical Journal 35, no. 6 (1998): 1004–1017. doi:10.1139/cgj-35-6-1004.

[6] Hsiung, Bin-Chen Benson. "A Case Study on the Behaviour of a Deep Excavation in Sand." Computers and Geotechnics 36, no. 4 (May 2009): 665–675. doi:10.1016/j.compgeo.2008.10.003.

[7] Hu, Z F, Z Q Yue, J Zhou, and L G Tham. "Design and Construction of a Deep Excavation in Soft Soils Adjacent to the Shanghai Metro Tunnels." Canadian Geotechnical Journal 40, no. 5 (October 2003): 933–948. doi:10.1139/t03-041.

[8]Korff, Mandy, Robert J. Mair, and Frits A. F. Van Tol. "Pile-Soil Interaction and Settlement Effects Induced by Deep Excavations." Journal of Geotechnical and Geoenvironmental Engineering 142, no. 8 (August 2016): 04016034. doi:10.1061/(asce)gt.1943-5606.0001434.

[9] Lee, C J, and N g, C W W. "Development of down drag on piles and pile groups in consolidating soil". Journal of Geotechnical and Geoenvironmental Engineering, ASCE; 130 (February 2004): 905-914. doi: 10.1061/(asce)1090-0241(2004)130:9(905).

[10] Leung, C F, Chow, Y K, and Shen, R F. "Behavior of pile subject to excavation-induced soil movement". Journal of Geotechnical and Geoenvironmental Engineering, ASCE; 126 (November 2000): 947-954. doi: 10.1061/(asce)1090-0241(2000)126:11(947).

[11] Leung, C F, Lim, J K, Shen, R F, and Chow, Y K. "Behavior of pile groups subject to excavation-induced soil movement". Journal of Geotechnical and Geoenvironmental Engineering, ASCE; 129 (January 2003): 58-65. doi:10.1061/(asce)1090-0241(2003)129:1(58).

[12] Leung, C F, Ong, DEL., Shen, R F., and Chow, Y K. "Pile behavior due to excavation-induced soil movement in clay II: Collapsed wall". Journal of Geotechnical and Geoenvironmental Engineering, ASCE; 132 (January 2006): 45-53. doi.org/10.1061/(asce)1090-0241(2006)132:1(45).

[13] Liu, Guang, Ming Cai, and Ming Huang. "Mechanical Properties of Brittle Rock Governed by Micro-Geometric Heterogeneity." Computers and Geotechnics 104 (December 2018): 358–372. doi:10.1016/j.compgeo.2017.11.013.

[14] Liyanapathirana, D.S., and R. Nishanthan. "Influence of Deep Excavation Induced Ground Movements on Adjacent Piles." Tunnelling and Underground Space Technology 52 (February 2016): 168–181. doi:10.1016/j.tust.2015.11.019.

[15] Mašín, D. "A Hypoplastic Constitutive Model for Clays." International Journal for Numerical and Analytical Methods in Geomechanics 29, no. 4 (2005): 311–336. doi:10.1002/nag.416.

[16] Mašín, David, and Ivo Herle. "State Boundary Surface of a Hypoplastic Model for Clays." Computers and Geotechnics 32, no. 6 (September 2005): 400–410. doi:10.1016/j.compgeo.2005.09.001.

[17] Mašín, David. "3D Modeling of an NATM Tunnel in High K0 Clay Using Two Different Constitutive Models." Journal of Geotechnical and Geoenvironmental Engineering 135, no. 9 (September 2009): 1326–1335. doi:10.1061/(asce)gt.1943-5606.0000017.

[18] Ng, Charles WW, B Simpson, M L Lings, and DFT Nash. "Numerical Analysis of a Multipropped Excavation in Stiff Clay." Canadian Geotechnical Journal 35, no. 1 (February 1998): 115–130. doi:10.1139/t97-074.

[19] Ng, C W W, Yau, T L Y, Li, J H M, and Tang, W H. "New failure load criterion for large diameter bored piles in weathered geomaterials". Journal of Geotechnical and Geoenvironmental Engineering, ASCE; 127 (June 2001): 488-498. doi:10.1061/(ASCE)1090-0241(2001)127:6(488)

[20] NG, C.W.W., Y. HONG, G.B. LIU, and T. LIU. "Ground Deformations and Soil–structure Interaction of a Multi-Propped Excavation in Shanghai Soft Clays." Géotechnique 62, no. 10 (October 2012): 907–921. doi:10.1680/geot.10.p.072.

[21] Ng, Charles W. W., Jiaqi Wei, Harry Poulos, and Hanlong Liu. "Effects of Multipropped Excavation on an Adjacent Floating Pile." Journal of Geotechnical and Geoenvironmental Engineering 143, no. 7 (July 2017): 04017021. doi:10.1061/(asce)gt.1943-5606.0001696.

[22] Nishanthan, Ravintharakumaran, D. S. Liyanapathirana, and Chin Jian Leo. "Shielding Effect in Pile Groups Adjacent to Deep Unbraced and Braced Excavations." International Journal of Geotechnical Engineering (July 8, 2016): 1–13. doi:10.1080/19386362.2016.1200270.

[23] Ong, DEL, Leung, C F, and Chow, Y K. "Pile behavior due to excavation-induced soil movement in clay". I: Stable Wall. Journal of Geotechnical and Geoenvironmental Engineering, ASCE; 132 (January 2006): 36-44. doi:10.1061/(ASCE)1090-0241(2006)132:1(36).

[24]Ong, DEL, Leung, C F, and Chow, Y K. "Behavior of pile groups subject to excavation-induced soil movement in very soft clay". Journal of Geotechnical and Geoenvironmental Engineering, ASCE; 135 (October 2009): 1462-1472. doi.org/10.1061/(asce)gt.1943-5606.0000095.

[25] Poulos H G, and Chen L T. "Pile response due to excavation-induced lateral soil movement". J Geotech Geoenviron Eng; 123 (February 1997): 94-99. doi:10.1061/(ASCE)1090-0241(1997)123:2(94).

[26] Soomro, Mukhtiar Ali, Dildar Ali Mangnejo, Riaz Bhanbhro, Noor Ahmed Memon, and Muneeb Ayoub Memon. "3D Finite Element Analysis of Pile Responses to Adjacent Excavation in Soft Clay: Effects of Different Excavation Depths Systems Relative to a Floating Pile." Tunnelling and Underground Space Technology 86 (April 2019): 138–155. doi:10.1016/j.tust.2019.01.012.

[27] Zhang, Runhong, Wengang Zhang, and Anthony Teck Chee Goh. "Numerical Investigation of Pile Responses Caused by Adjacent Braced Excavation in Soft Clays." International Journal of Geotechnical Engineering (September 6, 2018): 1–15. doi:10.1080/19386362.2018.1515810.

[28] Shakeel, M., and Charles W.W. Ng. "Settlement and Load Transfer Mechanism of a Pile Group Adjacent to a Deep Excavation in Soft Clay." Computers and Geotechnics 96 (April 2018): 55–72. doi:10.1016/j.compgeo.2017.10.010.